RUTHENIUM(0) NANOPARTICLES SUPPORTED ON BARE OR SILICA COATED FERRITE AS HIGHLY ACTIVE, MAGNETICALLY ISOLABLE AND REUSABLE CATALYST FOR HYDROGEN GENERATION FROM THE HYDROLYSIS OF AMMONIA BORANE

A THESIS SUBMITTED TO
THE GRADUATE SCHOOL OF NATURAL AND APPLIED SCIENCES
OF
MIDDLE EAST TECHNICAL UNIVERSITY

BY

ESRA SARICA

IN PARTIAL FULFILLMENT OF THE REQUIREMENTS
FOR
THE DEGREE OF MASTER OF SCIENCE
IN
CHEMISTRY

JULY 2019

Approval of the thesis:

RUTHENIUM(0) NANOPARTICLES SUPPORTED ON BARE OR SILICA COATED FERRITE AS HIGHLY ACTIVE, MAGNETICALLY ISOLABLE AND REUSABLE CATALYST FOR HYDROGEN GENERATION FROM THE HYDROLYSIS OF AMMONIA BORANE

submitted by **ESRA SARICA** in partial fulfillment of the requirements for the degree of **Master of Science in Chemistry Department, Middle East Technical University** by,

Prof. Dr. Halil Kalıpçılar
Dean, Graduate School of **Natural and Applied Sciences** _____

Prof. Dr. Cihangir Tanyeli
Head of Department, **Chemistry** _____

Prof. Dr. Saim Özkar
Supervisor, **Chemistry, METU** _____

Examining Committee Members:

Prof. Dr. Ahmet M. Önal
Chemistry, METU _____

Prof. Dr. Saim Özkar
Chemistry, METU _____

Assoc. Prof. Dr. Emren Nalbant Esentürk
Chemistry, METU _____

Assist. Prof. Dr. Salih Özçubukçu
Chemistry, METU _____

Prof. Dr. İzzet Morkan
Chemistry, Abant İzzet Baysal Üniversitesi _____

Date: 12.07.2019

I hereby declare that all information in this document has been obtained and presented in accordance with academic rules and ethical conduct. I also declare that, as required by these rules and conduct, I have fully cited and referenced all material and results that are not original to this work.

Name, Surname: Esra Sarıca

Signature:

ABSTRACT

RUTHENIUM(0) NANOPARTICLES SUPPORTED ON BARE OR SILICA COATED FERRITE AS HIGHLY ACTIVE, MAGNETICALLY ISOLABLE AND REUSABLE CATALYST FOR HYDROGEN GENERATION FROM THE HYDROLYSIS OF AMMONIA BORANE

Sarıca, Esra
Master of Science, Chemistry
Supervisor: Prof. Dr. Saim Özkar

July 2019, 33 pages

Ruthenium(0) nanoparticles supported on bare or silica-coated magnetite are prepared by impregnation of ruthenium(III) ions on the surface of support followed by their reduction with aqueous solution of sodium borohydride. The materials are magnetically isolated from the reaction solution and characterized by a combination of advanced analytical techniques including ICP-OES, BET, XRD, SEM-EDS, TEM, XPS. These magnetically isolable nanoparticles are used as catalyst in hydrogen generation from the hydrolysis of ammonia borane at room temperature. Ruthenium(0) nanoparticles, supported on bare magnetite and silica-coated magnetite, are highly active catalyst providing turnover frequency values of 29 and 127 min^{-1}, respectively, in hydrogen generation from the hydrolysis of ammonia borane at 25 °C. Thus, coating of the surface of magnetite with silica results in a significant enhancement in catalytic activity of ruthenium(0) nanoparticles in hydrogen generation from the hydrolysis of ammonia borane. Ruthenium(0) nanoparticles, supported on the silica coated magnetite, are also highly reusable as they preserve their initial catalytic activity even after the fifth reuse in hydrogen generation from the hydrolysis reaction.

Keywords: Magnetite; Silica Coating; Ruthenium; Ammonia Borane; Hydrogen Generation

ÖZ

AMONYAK BORAN HİDROLİZİNDEN HİDROJEN ÜRETİMİ İÇİN ETKİNLİĞİ YÜKSEK, MANYETİK OLARAK AYRILABİLİR VE YENİDEN KULLANILABİLİR KATALİZÖR OLARAK ÇIPLAK VEYA SİLİKA KAPLI DEMİR OKSİT YÜZEYİNE TUTUNMUŞ RUTENYUM(0) NANOKÜMELER

Sarıca, Esra
Yüksek Lisans, Kimya
Tez Danışmanı: Prof. Dr. Saim Özkar

Temmuz 2019, 33 sayfa

Çıplak veya silika kaplı manyetit yüzeyine tutunmuş rutenyum(0) nanokümeleri, rutenyum(III) iyonlarının, destek yüzeyine emdirilmesi ve ardından sulu sodyum borohidrür çözeltisi ile indirgenmesiyle hazırlandı. Oluşan malzemeler, tepkime çözeltisinden manyetik olarak ayrıldı ve ICP-OES, BET, XRD, SEM-EDS, TEM, XPS dahil olmak üzere ileri analitik tekniklerin bir kombinasyonu ile karakterize edildi. Bu manyetik olarak izole edilebilir nanoparçacıklar, oda sıcaklığında amonyak boran hidrolizinden hidrojen oluşumunda katalizör olarak kullanıldı. Çıplak ve silika kaplı manyetit yüzeyine tutulu rutenyum(0) nanoparçacıkları, sırasıyla 25.0 ± 0.1 °C'de amonyak boranının hidrolitik dehidrojenasyonunda 29 ve 127 dak^{-1} çevrim frekansı değerleri sağlayan oldukça aktif katalizörlerdir. Bu nedenle, manyetit yüzeyinin silika ile kaplanması, amonyum boran hidrolizinden hidrojen oluşumunda rutenyum(0) nanoparçacıklarının katalitik aktivitesinde önemli bir artışa neden olur. Silika kaplı manyetit üzerine tutturulan rutenyum(0) nanoparçacıkları ayrıca, hidroliz reaksiyonundan hidrojen oluşumunda beşinci kez yeniden kullanımdan sonra bile ilk katalitik aktivitelerini korudukları için yüksek oranda yeniden kullanılabilmektedir.

.

Anahtar Kelimeler: Manyetit; Silika Kaplama; Rutenyum; Amonyak Boran; Hidrojen Üretimi

To My Family

ACKNOWLEDGEMENTS

I would like to express my gratitude to my supervisor Prof. Dr. Saim Özkar for his valuable support, guidance and encouragement during this study. Without all the assistance and help, this work would have not been accomplished.

My special thanks to Assoc. Prof. Dr. Serdar Akbayrak for his endless support to make most of the characterization of the catalysts for this dissertation and other studies during my study.

My friend and laboratory collaborator, Elif Betül Kalkan is very appreciated for her support and precious friendship, not only during these studies but also in good times and in bad, in sickness and in health.

Thanks also extended to Prof. Dr. Yalçın Tonbul, Derya Özhava, Seda Tanyıldızı and all other members in 'Sozkar Research Group' for their good friendship, scientific collobrations, endless help and motivation.

The last but not the least, my special and sincere thanks go to my whole family and my dear friends for their endless love, invaluable support and considerations in every moment of my life.

TABLE OF CONTENTS

LIST OF TABLES

TABLES

LIST OF FIGURES

FIGURES

LIST OF ABBREVIATIONS

AB: Ammonia Borane

EIA: Energy Information Administration

ICP-OES: Inductively Coupled Plasma Optical Emission Spectroscopy

MOF: Metal Organic Framework

NP: Nanoparticle

P-XRD: Powder X-Ray Diffraction

SEM: Scanning Electron Microscope

SEM/EDS: Scanning Electron Microscope Electron Diffraction X-Ray

TEM: Transmission Electron Microscopy

TOF: Turnover Frequency

TON: Turnover Number

XPS: X-Ray Photoelectron Spectroscopy

CHAPTER 1

INTRODUCTION

1.1. Matter of Hydrogen

Energy demand increases day by day with economic growth and rising population [1]. Energy is a significant source in order to satisfy needs, develop standards of living and enhance human health and welfare. Hence, it has wide area of utilization. Electric power, transportation, residential, industrial and commercial sectors are the primary ones. Although there are alternative renewable energy sources (bioenergy, hydropower, wind, solar, geothermal and wood), petroleum, natural gas and coal as energy sources have a large share according to the U.S Energy Information Administration (EIA) report (Figure 1) [2].

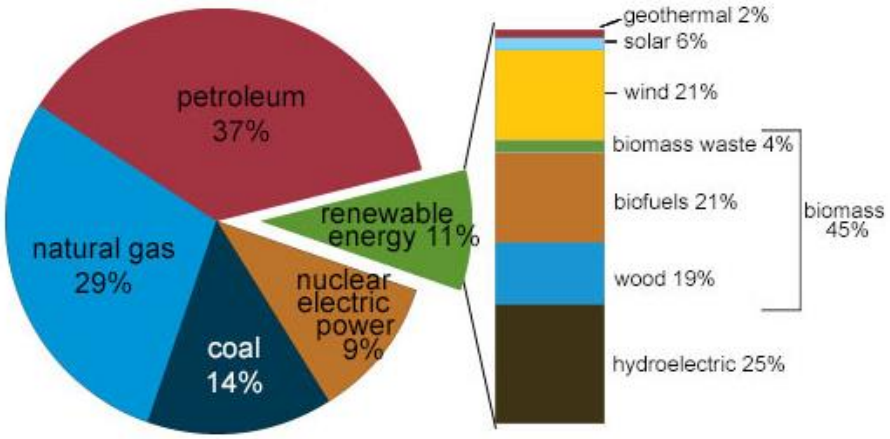

Figure 1.1. Place of Renewable Energy in Total Energy Sources [2]

The burning of fossil fuels, used to produce electricity continuously, causes rise of gas emission like methane, carbon dioxide and nitrous oxides in the atmosphere which results in environmental problems like global warming [3,4]. For fighting against the environmental hazards, using renewable energy sources is a significant remedy. As a

result, production of renewable energy has been growing rapidly during the recent years. In 2017, 11 % of the primary energy supply composed of renewable energy was reported by EIA as seen from the (Figure 1.1.). However, renewable energy sources throw up some new problems. One of them is the mismatch between energy consumption and generation. For instance, solar energy can provide the required electricity only at daytime, but the generating electricity from solar source is not possible during night. Hence, energy storage is a vital part for the active use of renewable energy sources. Also, the storage volume is important as well as storage for mobile applications. Fuel cell and hydrogen technologies play an important role at the energy system reducing greenhouse gas emissions, improving air quality and solving the problems that sustainable energy brings. For transition from fossil fuels to the renewable energy sources, hydrogen is seen to be the most promising energy carrier en route a sustainable energy future. Hence, term of 'hydrogen economy' has been found out, which is a proposed system delivering energy with hydrogen [5]. This was supported in the 2015 Paris Agreement by a considerable step to cope with climate change. The Hydrogen Council bring together thirteen world giant companies from the different sectors such as automotive, industrial and energy to propose a viable solution empowering the active usage of hydrogen, key solution for the energy transition, in Davos 2017 [6].

The reason of focusing on hydrogen is that it meets the demand for a clean and sustainable energy supply [7]. Hydrogen is regarded as a major energy carrier to be a remedy for environmental pollution and energy crisis because it is environmentally friendly and it has larger energy capacity unlike fossil fuels, which are responsible for the rise in concentration of the carbon dioxide in the atmosphere. However, hydrogen isn't used as the major fuel in today's conditions as a result of some obstacles. Storage, distribution and production problems can be examples of these obstacles. The reason of production problem can be explained as that hydrogen only occurs in the form of hydrocarbons and water on earth [8]. There are some ways for production of hydrogen. It can be provided with thermochemical, photo electrochemical and electrochemical

technologies by solar energy. Although these are special technologies for the energy requirement, these can be used only for immediate energy needs and special applications due to its high cost [9].

1.2. Hydrogen Storage

For the future hydrogen economy, the storage problem, the biggest obstacle to the common use of hydrogen, should be solved. Despite the difficulty of the hydrogen storage problem, some remarkable solutions can be a remedy. Three main methods have been explored in order to store hydrogen. The first one is high pressure tanks. Usage of high pressure tanks is simpler method. However, hydrogen has a low energy density by volume so that storage at higher ranges is possible with higher pressure. The required higher pressure poses disadvantage because of safety problem and also it is not practical for usage of mobile applications [10, 11].

Secondly, hydrogen can be stored in liquid form. Comparing with gas form, liquid has lower pressure with higher energy density. But, it also has drawback because of that liquefying hydrogen is an expensive process [11].

The last one is to use hydrogen-rich materials which have high gravimetric and volumetric hydrogen storage capacity [11]. Boron and nitrogen based compounds are considered as potential hydrogen storage materials because of their high contents of hydrogen and safety concerns. Ammonia borane, NH_3BH_3 is a stunning example for applications of chemical hydrogen storage due to its high stability in common solvents such as water and methanol, high gravimetric hydrogen content of 19.6% wt., low molecular weight (30.7 g mol^{-1}) and safe and controllable release of H_2 [12, 13]. These properties make ammonia borane one of the most promising hydrogen storage materials (Figure 1.2.) [14].

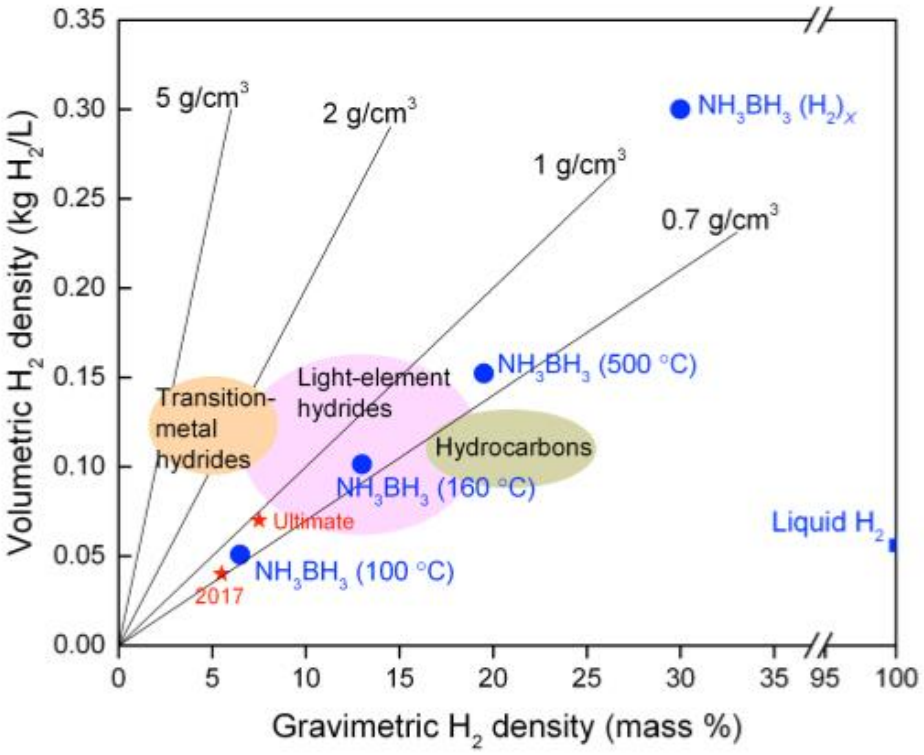

Figure 1.2. Comparison of gravimetric and volumetric H_2 densities of various hydrogen storage [14].

Hydrogen capacity of ammonia borane is higher than $LiBH_4$ (18wt%), N_2H_4 (12,6wt%) and $Mg(BH_4)_2$ (13,7wt%) [15,16]. Synthesis and characterization of ammonia borane were first reported by Sheldon Shore in the 1950s [17]. In NH_3BH_3, both B and N, light elements, are capable of bonding with H atoms. Bonds of N-H and B-H tend to be protonic and hydridic in turn, respectively, which lead to easy release of hydrogen gas [14].

1.3. Hydrogen Release from Ammonia Borane

Ammonia borane, rich in hydrogen, has the structure of colorless tetragonal molecular crystal under ambient conditions and it also has high solubility in water and other polar solvents [14]. Density of ammonia borane is 0.74 g/cm^3 and its melting point is in the range of 110-125 ºC depending on its purity. In the mid-1950s, AB was synthesized

firstly during developing boron hydride based fuels with high-energy for rockets and jets [18]. Most importantly, AB is stable, nontoxic, environmentally sound, and utilizable safely under environmental conditions. Hydrogen can be released from AB by thermolysis in solid state and in protic solvents, both of which need to be catalyzed [19]. Hydrogen release from thermal dehydrogenation of AB has been reported as a remarkable work [17]. For the release of higher amount of hydrogen in thermolysis, high temperature is required. But, high temperature causes formation of side products such as borazine. Thermal decomposition of AB only occurs at high temperatures under favour of its high stability. When the temperature is reduced, the sum of unwanted byproducts is also reduced but at the same time hydrogen production decreases. That is, temperature is a problem due to difficulty of reaction control. In contrast, catalytic solvolysis provides more favorable way for hydrogen producing from AB. Especially; catalytic hydrolysis is the most significant one for the hydrogen storage. The hydrogen generation from ammonia borane can be provided by catalytic hydrolysis in the presence of suitable catalysts [20]. At room temperature, hydrolysis of AB occur at appreciable rates only in the presence of suitable catalysts releasing 3 mole of H_2 per mole of ammonia borane [19,21] (Eq. 1).

$$NH_3BH_3(aq) + 2H_2O(l) \rightarrow NH_4^+(aq) + BO_2^-(aq) + 3H_2(g) \quad (1)$$

Obtaining 3 equivalent of hydrogen is more promotive process. However, developing effective and economical catalysts in order to improve the kinetic properties under the mild-conditions of reaction is one of the major defects of catalytic hydrolysis [20]. The transition metal nanoparticles are used commonly in catalysis because of their large fraction of surface atoms which lead to over catalytic activity when compared to the bulk metal. Transition metal nanoparticles provide high selectivity and activity in chemical reactions. On the date of 2006, Xu's group found the activity of noble metal nanocatalysts such as Rh [22,23], Ru [24], Pd [25] and Au for hydrolytic dehydrogenation of AB. Among the transition metal nanoparticles, ruthenium is the most widely investigated catalyst for both heterogeneous and homogeneous

dehydrogenation processes because of excellent catalytic features such as very-high activity [24] and reusability [26].

The problem encountered in the use of transition metal nanoparticles as catalyst is their tendency to agglomerate to larger particles and ultimately to the bulk metal, which is thermodynamic sink of metal. That high surface energy of metal nanoparticles agglomerates them in the form of large particles in default of stabilizing agents. Hence, ruthenium nanoparticles supported on the surface of porous materials such as zeolites [27] and metal organic frameworks (MOFs) [28], carbonecous materials such as active carbon [29], carbon nanotube [30], graphene [31]) or oxide supports such as titania TiO_2 [24], alumina Al_2O_3 [32], silica SiO_2 [33], ceria CeO_2 [34]) are highly active catalyst in hydrogenation from the hydrolysis of AB. Nevertheless, further enhancement in reusability of ruthenium catalyst is still a challenge. In this respect, magnetically recoverable catalysts have been of top priority since magnetic property provides easier separation from the reaction solution compared to the filtration and centrifugation techniques [35]. Catalyst can be separated and recycled easily by combining magnetic nanoparticles with catalytically active part [36]. Cobalt, iron and nickel are recyclable and active catalysts. Unfortunately, a few metals have magnetic properties and their oxides are catalytically active for limited reactions. Among oxides, iron oxide nanoparticles (Fe_2O_3 and Fe_3O_4) have been performed in various reactions like hydrogenation, oxidative and coupling reactions [37,38], on top of generating hydrogen by the AB hydrolysis. For this reason, in this study, magnetite (Fe_3O_4) was used as magnetic support for ruthenium(0) nanoparticles.

Another issue in using magnetic powders as supports is uncontrolled involvement of the metal component such as iron in the catalytic reaction. To prevent unruly involvement of iron, the surface of magnetite (Fe_3O_4) can be modified by coating with inert materials such as silica [33] or polymer [39,40]. Thanks to these materials, magnetic powders and metal nanoparticles have controllable size and size distribution. Hence, the surface of magnetite has been coated with the silica (SiO_2), preventing the

uncontrollable aggregation and providing the stability for the ruthenium(0) nanoparticles. In addition to providing stabilization of metal nanoparticles against agglomeration, silica coating can also hinder the involvement of iron in the catalytic reaction. In this dissertation, magnetite nanopowders were used as magnetic support for the ruthenium(0) nanoparticles. In order to prevent the involvement of iron in the catalytic reaction, magnetite nanopowders were coated by a silica layer. Thus, magnetically separable Fe_3O_4 and SiO_2-Fe_3O_4 were used as support for Ru NP catalysts in the hydrogen generation from the hydrolysis of ammonia borane under mild conditions. The magnetically isolable ruthenium(0) nanoparticles supported on magnetite (Ru^0/Fe_3O_4) and ruthenium(0) nanoparticles supported on the silica coated magnetite (Ru^0/SiO_2-Fe_3O_4) catalysts were prepared by impregnation of ruthenium(III) ions on the surface of support from the aqueous solution followed by reduction with sodium borohydride. The magnetically isolable Ru^0/Fe_3O_4 and Ru^0/SiO_2-Fe_3O_4 catalysts could easily be isolated from the reaction solution by using a permanent magnet and characterized by ICP-OES, XRD, TEM, SEM-EDS and XPS techniques. The magnetically isolable Ru^0/Fe_3O_4 and Ru^0/SiO_2-Fe_3O_4 catalysts were found to be highly active catalyst in hydrogen generation from the hydrolysis of ammonia borane at ambient temperature, releasing 3 mol H_2 per mole of ammonia borane. More importantly, the magnetically isolable Ru^0/Fe_3O_4 and Ru^0/SiO_2-Fe_3O_4 nanoparticles are highly reusable catalyst for hydrolytic dehydrogenation of ammonia borane.

CHAPTER 2

EXPERIMENTAL

2.1. Materials

Ruthenium(III) chloride trihydrate ($RuCI_3.3H_2O$), magnetite nanopowder (Fe_3O_4, 97%), tetraethylorthosilicate (TEOS, 98%), ammonia borane (H_3NBH_3, 97%) and ammonium hydroxide (NH_4OH) were purchased from Aldrich. In addition, Sodium borohydride ($NaBH_4$, 98%) was purchased from Merck.

2.2 Preparation of silica coated magnetite (SiO_2-Fe_3O_4)

Silica coating was carried out following a modified Stöber process [41]. Concisely, Fe_3O_4 (800 mg) was put into a solution including 80 mL distilled water, 320 mL ethanol and 9.6 mL NH_4OH (%25) in a 500 mL round bottom flask at room temperature. This solution was ultrasonicated for 20 minutes and then, 4 mL TEOS in 10 mL ethanol was added drop wise to the magnetite suspension in the round bottom flask. This mixture was stirred mechanically in a rotary evaporator for 6 hours without evaporation at room temperature. After 6 h, silica coated magnetite (SiO_2-Fe_3O_4) were collected by a magnet and washed with 100 mL distilled water for five times and then dried overnight in the oven at 120 ºC.

2.3 Preparation of Ru^0/Fe_3O_4 and Ru^0/SiO_2-Fe_3O_4

The dried SiO_2-Fe_3O_4 (400 mg) was added to a solution of $RuCI_3.3H_2O$ (46.2 mg) in 50 mL H_2O in a beaker (Note that the amount of ruthenium salt was arranged according to the desired Ru loading). The mixture was sonicated for 15 min, and then stirred for 24 h at room temperature. Afterwards, aqueous solution of sodium borohydride (at the mol ratio of $NaBH_4$/Ru = 5) was added drop wise into the suspension. After 1 h stirring, the sample was isolated using a permanent magnet and

washed with distilled water and the residue was dried for 12 h at 60 ºC under vacuum. For comparing, Ru^0/Fe_3O_4 was also prepared by following the same procedure as identified above, using Fe_3O_4 in the place of SiO_2-Fe_3O_4. The samples were characterized by ICP-OES, TEM, SEM-EDX and XPS techniques as described in our recent report [42].

2.4 Hydrogen generation from the hydrolytic dehydrogenation of AB using Ru^0/Fe_3O_4 and Ru^0/SiO_2-Fe_3O_4 catalysts

The catalytic activity of Ru^0/Fe_3O_4 and Ru^0/SiO_2-Fe_3O_4 (4.0% wt Ru) catalyst were investigated by monitoring the H_2 evolution from the hydrolysis of AB using our established experimental set up [41]. In order to be able to determine the rate of hydrogen generation from the hydrolytic dehydrogenation of AB using Ru^0/Fe_3O_4 and Ru^0/SiO_2-Fe_3O_4 catalysts, a jacketed reaction flask containing a Teflon-coated stir bar was placed on a magnetic stirrer (WiseStir MSH-20A) and thermostated to 25.0 ± 0.1 °C by circulating water through its jacket from constant temperature bath. To observe the hydrogen gas evolution, a graduated glass tube filled with water was connected to the jacketed flask. Then, ruthenium(0) nanoparticles supported on the surface of bare magnetite or silica-coated magnetite nanopowders in 10 mL water were transferred into the jacketed reaction flask and stirred until it reached the thermal equilibrium. After that, 1.0 mmol (31.8 mg) of ammonia borane (NH_3BH_3) was added to the solution. The jacketed reaction flask was sealed by a septum to prevent the loss of gaseous components and stirred meanwhile the reaction was followed until there was no release of H_2 gas. Note that Fe_3O_4 and SiO_2-Fe_3O_4 supports have been shown to be catalytically inert in this reaction.

Figure 2.1. The experimental setup which used in performing the catalytic hydrolysis of ammonia borane and measuring the hydrogen generation rate. (1) water bath circulator, (2) magnetic stirrer, (3) jacketed schlenk tube, (4) water- in, (5) water- out, (6) plastic hose, (7) water filled burette.

2.5 Determination of the optimum Ru loading of Ru^0/SiO_2-Fe_3O_4 for the highest catalytic activity in the hydrolytic dehydrogenation of AB

Ru^0/SiO_2-Fe_3O_4 samples with different Ru contents (1-4% wt) were analyzed in hydrolysis of AB (100 mM) in 10 mL of H_2O at 25.0 ± 0.1 ºC by holding the Ru concentration constant. For catalytic hydrolysis of AB using Ru^0/SiO_2-Fe_3O_4 catalysts, the sample with 4.0% wt. Ru loading provides the highest activity in hydrolysis of AB. Therefore, Ru^0/SiO_2-Fe_3O_4 (4.0% wt. Ru) and Ru^0/Fe_3O_4 (4.0% wt. Ru) catalysts were used for all the characterizations and tests.

2.6 Determination of activation energy for hydrolytic dehydrogenation of AB catalyzed by Ru^0/Fe_3O_4 and Ru^0/SiO_2-Fe_3O_4

The hydrolytic dehydrogenation of AB was performed starting with 10 mL of 100 mM (31.8 mg) AB solution and 10 mg of Ru^0/SiO_2-Fe_3O_4 (4.0% wt. Ru) or Ru^0/Fe_3O_4 (4.0% wt. Ru) catalysts at various temperatures (25, 30, 35, 40 ºC) in order to determine the activation energy (E_a).

2.7 Reusability of Ru^0/Fe_3O_4 and Ru^0/SiO_2-Fe_3O_4 in hydrolytic dehydrogenation of AB

The reusability of catalysts was analyzed in the hydrolysis of 10 mL solution including 100 mM AB and 30 mg of Ru^0/SiO_2-Fe_3O_4 (4.0% wt. Ru) or Ru^0/Fe_3O_4 (4.0% wt. Ru) at 25.0 ± 0.1 ºC. When the first run is completed, while keeping the catalyst separated by a magnet in the bottom of flask, the reaction solution was replaced by a new batch of 10 mL solution of 100 mM AB. After releasing catalytic materials into the solution by removing the magnet, the next run of hydrolysis was started at 25.0 ± 0.1 ºC. This experiment was repeated at least five times in this manner and results were expressed as the percentage of initial catalytic activity in the successive hydrolysis of ammonia borane.

CHAPTER 3

RESULTS AND DISCUSSION

3.1. Preparation and Characterization of Ru^0/SiO_2-Fe_3O_4 and Ru^0/Fe_3O_4

Ru^0/SiO_2-Fe_3O_4 and Ru^0/Fe_3O_4, magnetically separable catalysts, were prepared by impregnation of Ru^{3+} ions on the surface of SiO_2-Fe_3O_4 or Fe_3O_4 pursued by their reduction with aqueous solution of sodium borohydride. The isolated catalysts were characterized by a combination of analytical techniques including XRD, ICP, TEM, SEM-EDX and XPS. Fig. 3.1 shows the XRD patterns of Fe_3O_4, Ru^0/Fe_3O_4, SiO_2-Fe_3O_4 and Ru^0/SiO_2-Fe_3O_4, which indicate that there is no variation in the diffraction patterns of Fe_3O_4 after coating the surface with silica or supporting ruthenium on the surface. Although ruthenium loading and silica coating could not be observed from the XRD analysis, one can observe that there is no change in the position of diffraction peaks of Fe_3O_4 after the formation of Ru NPs on the surface of magnetite nanopowders.

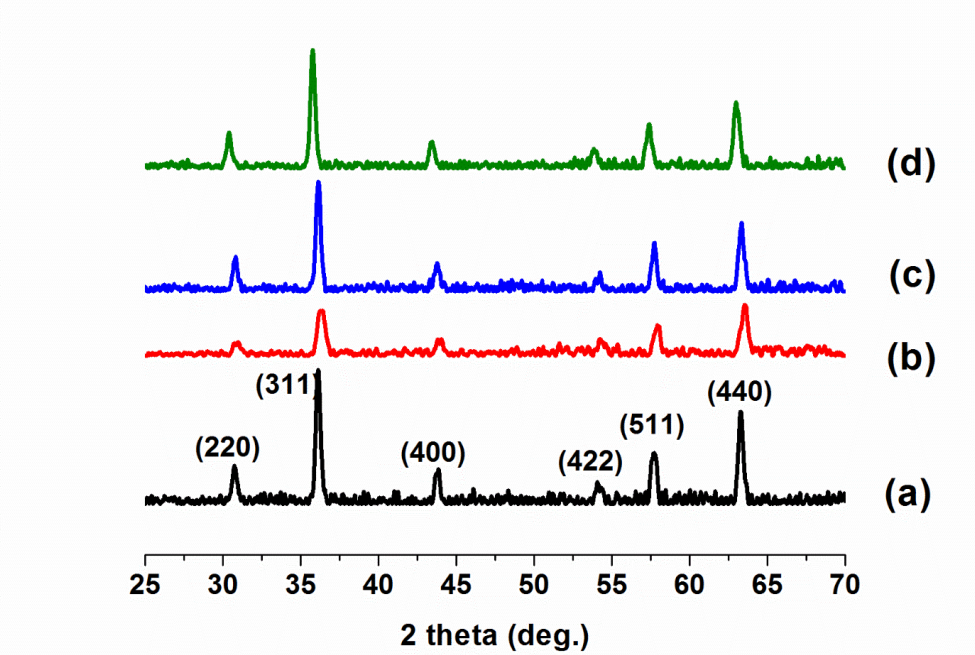

Figure 3.1. Powder XRD patterns of (a) Fe_3O_4, (b) Ru^0/Fe_3O_4 (4.0% wt. Ru), (c) SiO_2/Fe_3O_4, d) Ru^0/SiO_2- Fe_3O_4 (4.0% wt. Ru).

Inspection of the TEM images given in Fig. 3.2 reveals the followings: (i) Ru NPs are successfully anchored on the surface of Fe_3O_4 nanopowder (Fig. 3.2. b-c) and nanoparticles are well dispersed with an average particle size of 3.75 ± 0.81 nm (Fig. 3.2. d). (ii) Magnetite particles are covered by a silica layer of about 20 nm thickness (Fig. 3.2. e-g). (iii) Silica coating does encapsulate the magnetite particles, though a few of them under the same protective cover. The magnetite particles are not well separated during the coating process, rather agglomerating to clumps of very small number of particles, because of either relatively high concentration of Fe_3O_4 particles (800 mg per 400 mL solution) or intrinsic tendency of Fe_3O_4 particles for agglomeration in aqueous solution where weak hydrogen bonding can hold some of the particles close to each other, forming very small assemble. (iv) Ruthenium(0) NPs are well dispersed on the surface of silica layer (Fig. 3.2. e-g) and have an average particle size of 3.43 ± 0.69 nm (Fig. 3.2. h). That magnetite particles are successfully coated with a thick silica layer, which is expected to hinder the involvement of iron in the catalytic hydrolysis of AB is the most important observation. In this study, the

greatest success is that hiding the magnetic particles under the silica layer is on the way towards the synthesis of magnetically isolable metal nanoparticles used as reusable catalyst in hydrogen release from AB.

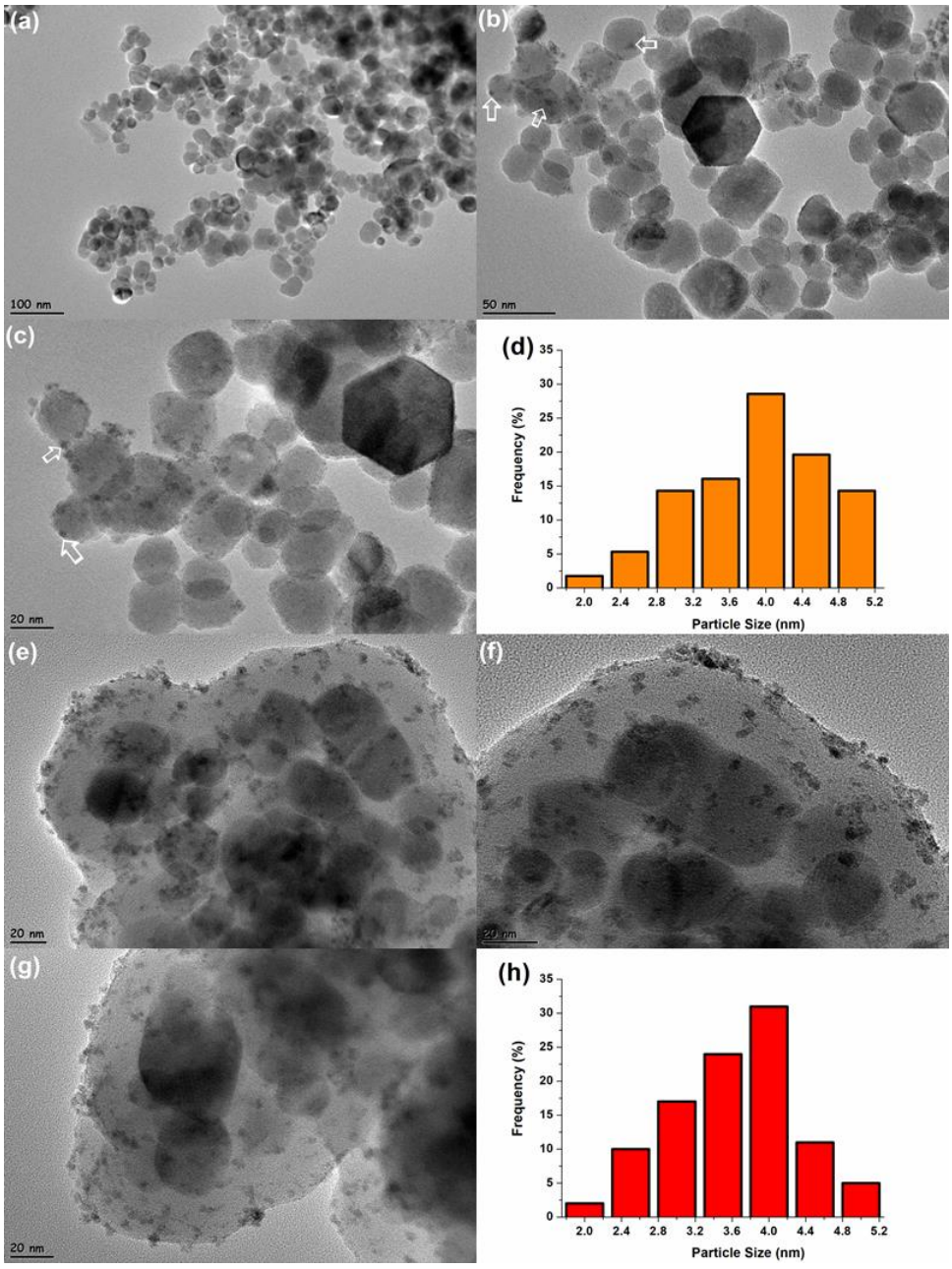

Figure 3.2. TEM images of a) Fe_3O_4, (b-c) Ru0/ Fe_3O_4 (4.0% wt Ru) and (d) the corresponding histogram. (e-g) TEM images of Ru^0/SiO_2-Fe_3O_4 (4.0% wt Ru) and (h) the corresponding histogram showing the particle size distribution.

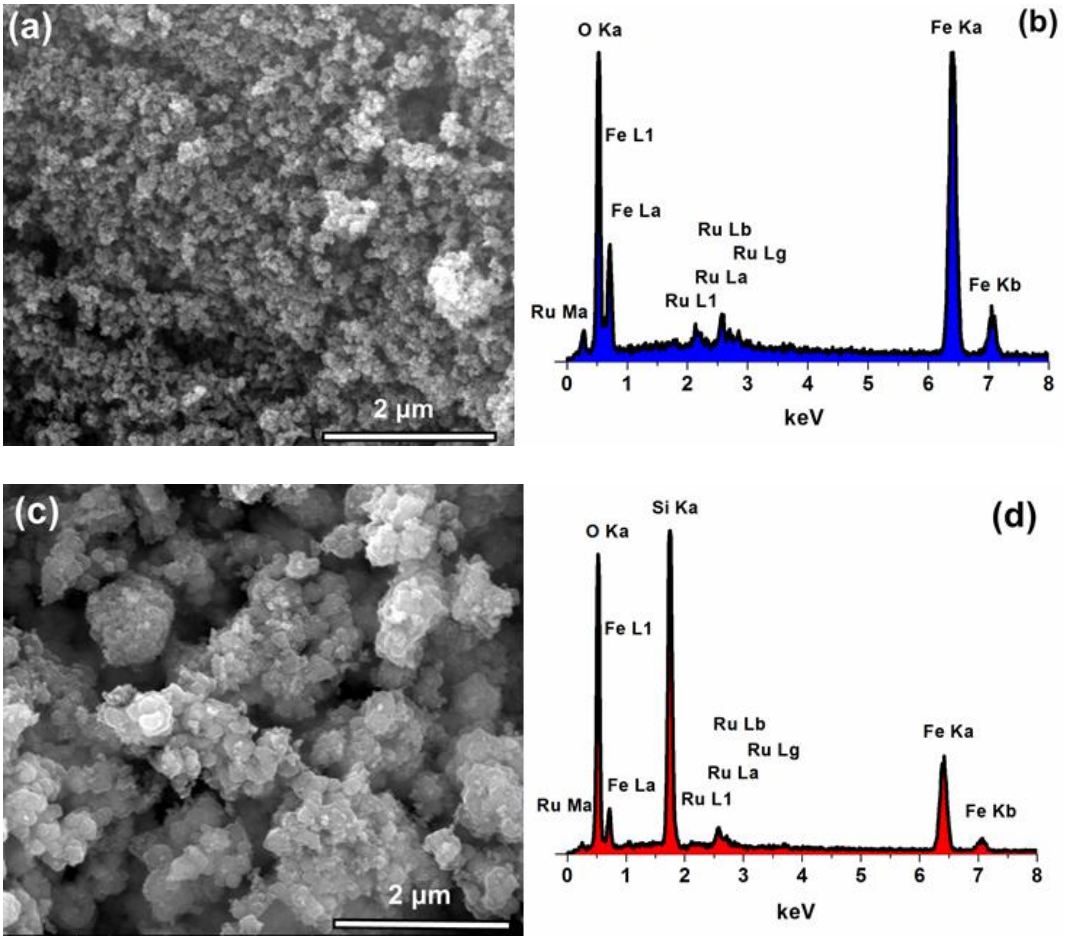

Figure 3.3. (a) SEM image of Ru^0/ Fe_3O_4 (4.0% wt Ru) and (d) EDX spectrum taken from a. (c) SEM image of Ru^0/ SiO_2- Fe_3O_4 (4.0% wt Ru) and (d) EDX spectrum taken from c.

The existence of Ru NPs on the surface of Fe_3O_4 and SiO_2-Fe_3O_4 were confirmed by SEM-EDX analysis. Indeed, SEM-EDX shows that Ru is the only element detected in addition to the framework elements of magnetite (Fe, O) (Fig 3.3. b), and silica coated magnetite (Si, Fe, O) (Fig. 3.3. d).

The composition of Ru^0/SiO_2-Fe_3O_4 and Ru^0/ Fe_3O_4 catalysts and the oxidation state of ruthenium metal were investigated by analysis of XPS. Fig. 3.4. a and Fig. 3.4. c represent the survey-scan XPS spectra of Ru^0/Fe_3O_4 and Ru^0/SiO_2-Fe_3O_4 samples, respectively, emphasizing the presence of Ru element in both of the Fe_3O_4 and SiO_2-Fe_3O_4 samples. The XPS peaks at 279.4 eV for Ru^0/Fe_3O_4 (Fig. 3.4. b) and Ru^0/SiO_2-Fe_3O_4 (Fig. 3.4. d) are assigned to the Ru^0 $3d_{5/2}$ bands [43]. The higher energy peaks

(282.5 eV, 284.5 eV, 287.1, 288.1 eV) are attributed to the C1s or Ru $3d_{3/2}$ since the overlaps with the C 1s and Ru $3d_{3/2}$ bands in that region.

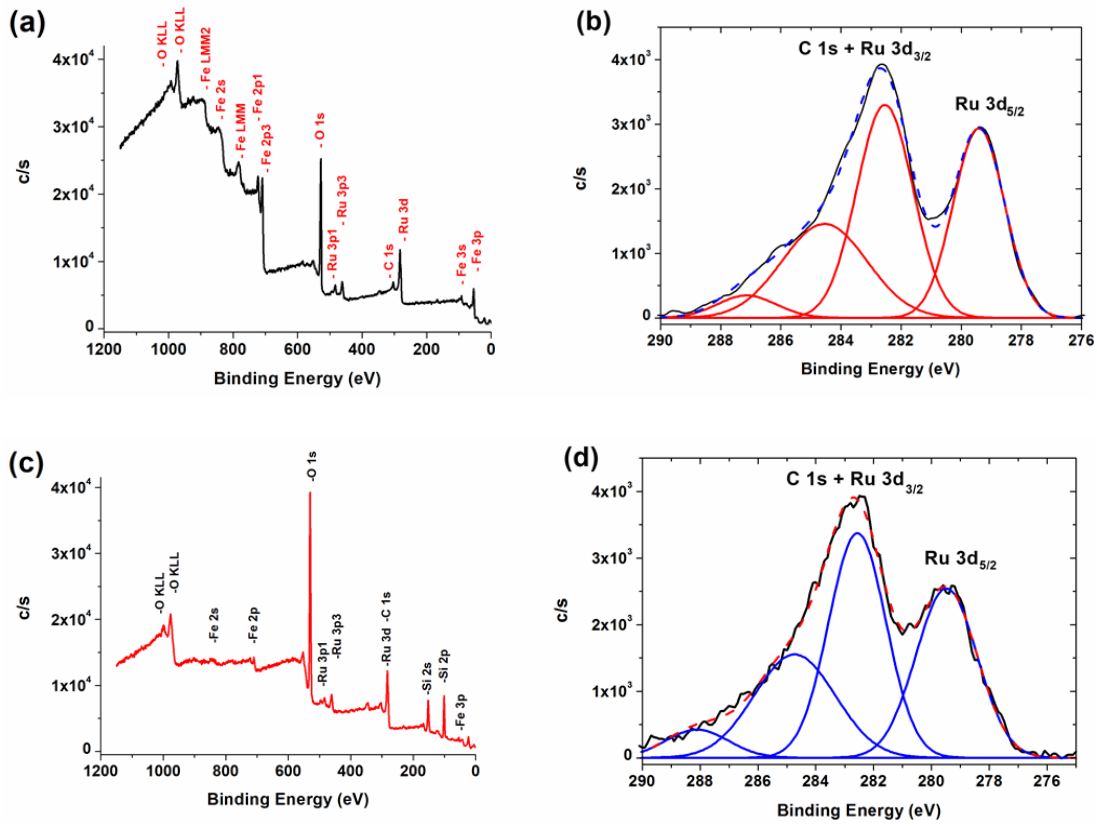

Figure 3.4. X-ray photoelectron spectrum of (a) Ru^0/Fe_3O_4 (4.0% wt Ru) and (b) Ru^0/SiO_2-Fe_3O_4 (4.0% wt Ru). The high resolution scan and deconvolution of Ru 3d bands of (b) Ru^0/Fe_3O_4 and (d) Ru^0/SiO_2-Fe_3O_4.

Previous to begin studying the hydrogen release from the hydrolysis of AB catalyzed by Ru(0) NPs on the surface of silica coated magnetite nanopowders Ru^0/Fe_3O_4 and Ru^0/SiO_2-Fe_3O_4, we performed control experiments to show SiO_2-Fe_3O_4 being catalytically silent in this reaction.

3.2. Catalytic Activity of Ru^0/Fe_3O_4 and Ru^0/SiO_2-Fe_3O_4 Nanoparticles in Hydrogen Generation from the Hydrolysis of Ammonia Borane

Expectedly, Ru(0) nanoparticles supported on the surface of bare magnetite or silica coated magnetite are found to be active catalyst in hydrolysis of AB. Fig. 3.5. shows the H_2 evolution versus time plots for the hydrolysis of AB (100 mM) using Ru^0/Fe_3O_4

and Ru^0/SiO_2-Fe_3O_4 catalysts both with 4.0%wt. Ru loading at 25.0 ± 0.1 ºC. In either case, H_2 release starts immediately after a short induction period less than 3 minutes and continues almost linearly until the completion of 3 equivalent H_2 evolution per mole of AB. As seen from Figure 3.5 a, the hydrogen generation rate for the Ru^0/SiO_2-Fe_3O_4 catalyst is higher than that for the Ru^0/Fe_3O_4 catalysts. This is the only distinguishable difference between two catalysts. This difference in activity can readily be attributed to the silica coating, which hides the magnetite core under thick cover. Thus, the negative effect of magnetite on the activity of Ru(0) NPs supported on the surface is hindered by the silica layer.

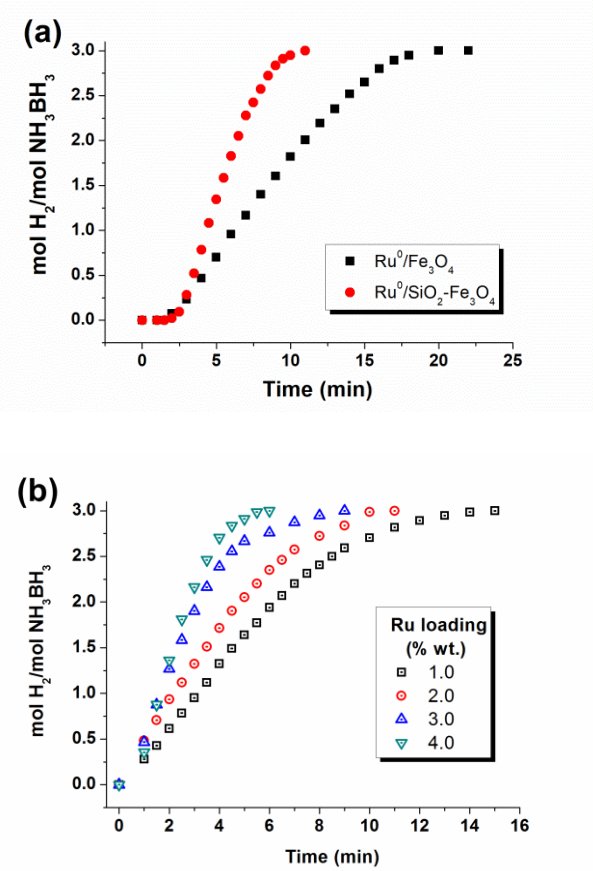

Figure 3.5. (a) Plot of mol H_2/mol NH_3BH_3 versus time for the hydrolytic dehydrogenation of AB (100 mM) starting with Ru^0/SiO_2-Fe_3O_4 or Ru^0/SiO_2-Fe_3O_4 catalysts both with 4.0%wt. Ru loading at 25.0 ± 0.1 ºC, (b) Plot of mol H_2/mol NH_3BH_3 versus time for the hydrolytic dehydrogenation of AB (100 mM) starting with Ru^0/SiO_2-Fe_3O_4 (0.79 mM Ru) with different Ru loading at 25.0 ± 0.1ºC.

To determine the optimum ruthenium loading of Ru^0/SiO_2-Fe_3O_4 catalysts for the highest catalytic activity in hydrolytic dehydrogenation of AB, additional control experiments were performed. Fig. 3.5. b shows the plots of equivalent H_2 versus time for the hydrolytic dehydrogenation of AB (100 mM) starting with Ru^0/SiO_2-Fe_3O_4 catalyst (0.79 mM Ru) with different ruthenium contents in the range 1.0-4.0% wt. Ru at 25.0 ± 0.1 ºC. The turnover frequency values (TOF) calculated from the hydrogenation in the linear part of plots are 42, 57, 101, and 127 min^{-1} for the Ru^0/SiO_2-Fe_3O_4 catalysts with 1.0, 2.0, 3.0 and 4.0% wt. Ru loading, respectively. Since the Ru^0/SiO_2-Fe_3O_4 (4.0% wt.) sample shows the highest catalytic activity, the catalyst with 4.0% wt. Ru was used for all the further experiments in this work.

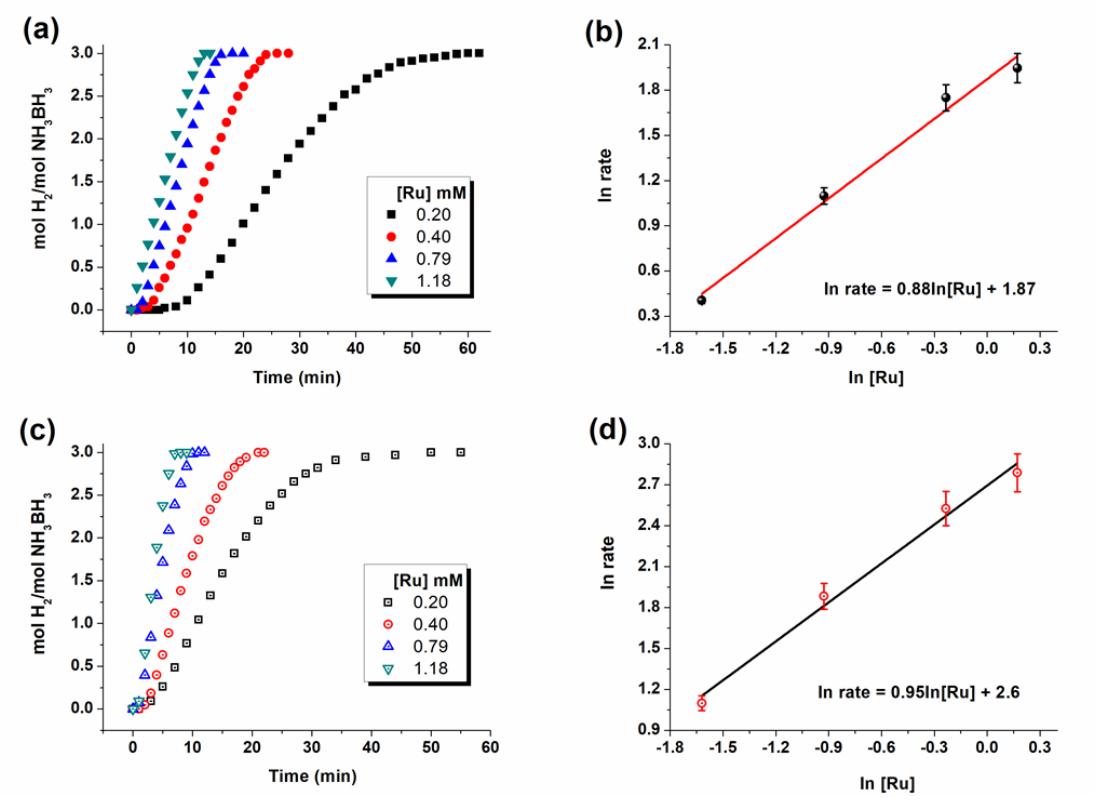

Figure 3.6. mol H_2/mol NH_3BH_3 versus time graph depending on the Ru concentration in (a) Ru^0/Fe_3O_4 (4.0% wt Ru) and (c) Ru^0/SiO_2-Fe_3O_4 (4.0% wt Ru) for the hydrolysis of AB (100 mM) at 25.0 ± 0.1°C. (b and d) The corresponding plots of hydrogen generation rate versus the concentration of Ru, both in logarithmic scale constructed from a and c, respectively.

Fig. 3.6. a and Fig. 3.6. c indicate the equivalent H_2 generated per mole of AB versus time graphs during the hydrolytic dehydrogenation of AB (100 mM) starting with Ru^0/Fe_3O_4 (4.0% wt Ru) or Ru^0/SiO_2-Fe_3O_4 (4.0% wt Ru) catalysts in different Ru concentration at 25.0 ± 0.1 ºC. The rate of H_2 generation was determined by the linear part of each plot in Fig. 3.6. a and Fig. 3.6. c and plotted versus ruthenium concentration, both in logarithmic scale. The resulting plots in Fig. 3.6. b and Fig. 3.6. d give linear lines with a slope of 0.88 and 0.95 for the Ru^0/Fe_3O_4 (4.0% wt Ru) and Ru^0/SiO_2-Fe_3O_4 catalysts, respectively, indicating that the hydrolysis of AB is first order with respect to the ruthenium concentration in both reactions. The initial TOF values of Ru^0/Fe_3O_4 (4.0% wt Ru) and Ru^0/SiO_2-Fe_3O_4 (4.0% wt Ru) are 29 and 127 min^{-1}, respectively, in hydrogen generation from the hydrolysis of AB at 25.0 ± 0.1 ºC. Recall that both of Ru^0/Fe_3O_4 (4.0% wt Ru) and Ru^0/SiO_2-Fe_3O_4 (4.0% wt Ru) catalysts have similar average particle sizes of Ru NPs, 3.75 ± 0.81 nm and 3.43 ± 0.81 nm, respectively. Thus, the high catalytic activity of Ru^0/SiO_2-Fe_3O_4 may be attributed to (i) the higher surface area of SiO_2-Fe_3O_4 (61 m^2/g) compared to that of Fe_3O_4 (44 m^2/g), (ii) the nature of silica surface as compared to magnetite, and (iii) the protective silica cover which prevents the negative effects of magnetite on the catalysis. In hydrolysis of AB, the catalytic activity of Ru^0/SiO_2-Fe_3O_4 catalysts is comparable to that of the reported catalysts listed in Table 1.

3.3. Kinetics of Ru^0/Fe_3O_4 and Ru^0/SiO_2-Fe_3O_4 Nanoparticles in Hydrogen Generation from the Hydrolysis of Ammonia Borane

The analysis of the hydrolytic dehydrogenation of AB at different temperatures in the range of 25-40 ºC using Ru^0/Fe_3O_4 (Fig. 3.7. a) and Ru^0/SiO_2-Fe_3O_4 (Fig. 3.7. c) catalysts were performed. The rate constants for the H_2 evolution reaction were determined from the slope in the linear part of each plot given Fig. 3.7.a and Fig. 3.7. c. The temperature dependent rate constants were used to construct the Arrhenius plots in Fig. 3.7. b and 3.7. d. The apparent activation energy (E_a) for the hydrolysis of AB using Ru^0/Fe_3O_4 and Ru^0/SiO_2-Fe_3O_4 catalysts is 77 ± 2 $kJ.mol^{-1}$ and 54 ± 2 $kJ.mol^{-1}$,

respectively. The E_a values for the Ru catalysts reported for the hydrolysis of AB are also listed in Table 3.1 for comparison. It is admirable that there is no correlation between catalytic activity and the activation energy as seen from Table 3.1.

Table 3.1. The turnover frequency (TOF; *mol H_2·(mol Ru)$^{-1}$.(min)$^{-1}$*), activation energy (E_a; *kJ.mol^{-1}*) and the reusability of Ru catalysts used in H_2 generation from the hydrolysis of ammonia borane. * The cases of recyclability where AB has been added into the reaction solution without separating the catalyst from the reaction mixture.

Catalyst	TOF (min^{-1})	Ru/AB molar ratio	E_a ($kJ.mol^{-1}$)	Reusability (% of retaining initial activity)	Ref.
Ru/TiO_2 (anatase+rutile)	604	0.001	37.7	-	[24]
Ru/graphene	600	0.002	12.7	*80% after 5.Run	[31]
Ru/TiO_2 (rutile)	510	0.001	-	-	[24]
Ru/TiO_2 (anatase)	455	0.001	-	-	[24]
Ru/Carbon black	429.5	0.00425	34.81	43.1% after 5.Run	[29]
Ru^0/CeO_2	361	0.00095	51	60% after 5.Run	[34]
Ru^0/MWCNT	329	0.00094	33	41% after 4.Run	[30]
Ru/SBA-15	316	0.002	34.8	-	[44]
Ru/g-C_3N_4	313	0.0017	37.4	50% after 4.Run	[45]
Ru/TiO_2(B) nanotube	303	0.0041	45.6	*25% after 4.Run	[46]
Ru-MIL 53(Al)	266.9	0.004	33.7	*75% after 5.Run	[28]
Ru-MIL 53(Cr)	260.8	0.004	28.9	*71% after 5.Run	[28]
Ru@TiO_2	241	0.0006	70	-	[47]
Ru@MIL-96	231	0.0039	48	*65% after 5.Run	[48]
Ru/nanodiamond	229	0.0033	50.7	40% after 5.Run	[49]
Ru@SiO_2	200	0.0025	38	-	[50]
Ru@MIL-101	178	0.008	51	-	[51]
Ru^0/ZrO_2	173	0.0063	58	67% after 5.Run	[52]
Ru(0)/SiO_2-$CoFe_2O_4$	172.5	0.00097	45.6	94% after 10.Run	[35]
Ru/HfO_2	170	0.00396	65	75% after 5.Run	[53]
Ru/Hap	137	0.00392	58	92% after 5.Run	[54]
Ru^0/X-NW	135	0.00271	77	-	[26]
RuCu/graphene	135	0.004	30.59	-	[55]
Ru^0/SiO_2-Fe_3O_4	127	0.0079	54	100% after 5.Run	This work
Commercial Ru/C (3.0%wt)	113	0.00178	76	-	[56]
Ru/graphene	100	0.010	11.7	*72% after 4.Run	[57]
Ru^0/ Fe_3O_4	29	0.0079	77	100% after 5.Run	This work
Nanoporous Ru ($Ru_{20}Al_{80}$)	26.7	0.01	66.5	*67% after 5.Run	[58]
Meta stable Ru NPs	21.8	0.00250	27.5	-	[59]

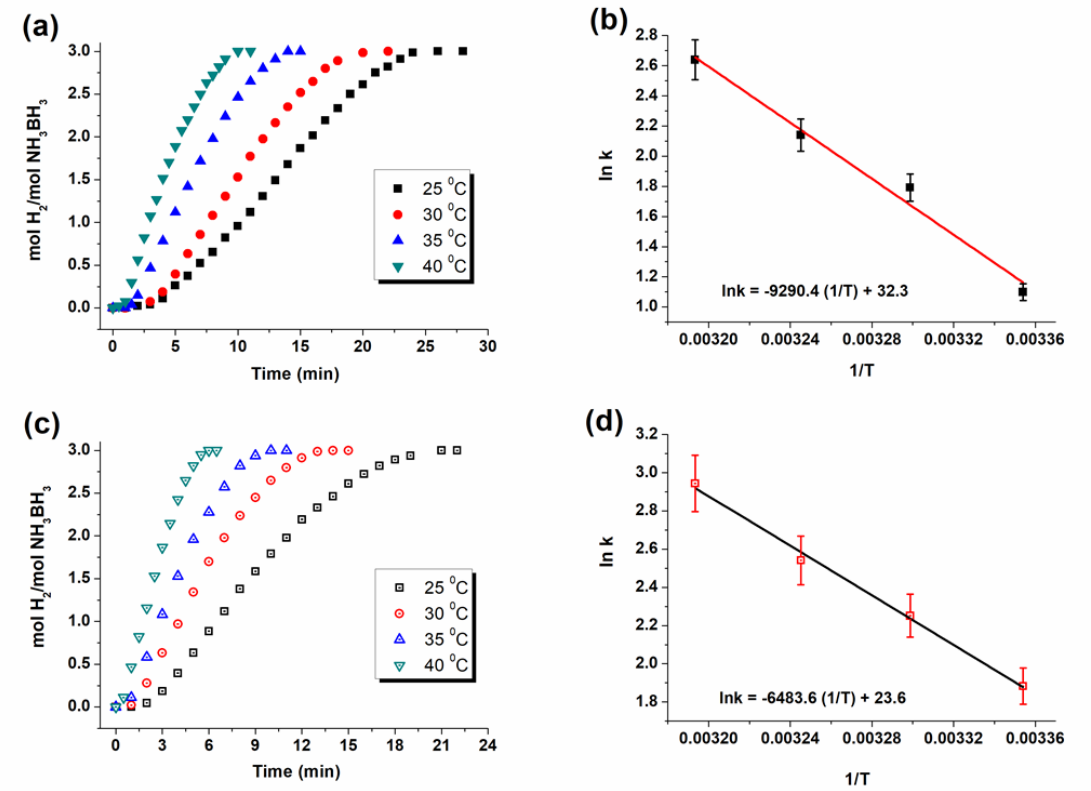

Figure 3.7. The evolution of equivalent H_2 per mole of AB versus time plot for the hydrolytic dehydrogenation of AB starting with (a) Ru^0/Fe_3O_4 (4.0% wt Ru; 0.40 mM Ru), (c) Ru^0/SiO_2- Fe_3O_4 (4.0% wt Ru; 0.40 mM Ru) and 100 mM AB at various temperatures. The corresponding Arrhenius plots for the (b) Ru^0/Fe_3O_4 and (d) Ru^0/SiO_2-Fe_3O_4, catalyzed hydrolytic dehydrogenation of AB.

3.4. Reusability of Ru^0/Fe_3O_4 and Ru^0/SiO_2-Fe_3O_4 Nanoparticles in the Hydrolysis of Ammonia Borane

The reusability of Ru^0/Fe_3O_4 and Ru^0/SiO_2-Fe_3O_4 catalysts were also studied in hydrolytic dehydrogenation of AB. The catalysts were subsequently used five times in this reaction by isolation of catalyst from the reaction solution using a permanent magnet after previous run and redispersing in a new batch of AB solution for the next run of hydrolysis. The resulting H_2 evolution plots (Fig. 3.8. a-b) and the plots of corresponding percent initial catalytic activity and the percent conversion of AB for each run (Fig. 3.8. c-d) demonstrate that there is no remarkable loss in the catalytic activity of Ru^0/Fe_3O_4 and Ru^0/SiO_2-Fe_3O_4 catalysts after five reuses and 100%

conversion of AB is succeed in all the cycles. Indeed, the isolated solution after each run provides no catalytic activity, which shows no leaching of Ru NPs to the reaction solution. Table 3.1. also gives the reusability behavior of the Ru catalysts reported for the hydrolysis of AB. The Ru^0/Fe_3O_4 and Ru^0/SiO_2-Fe_3O_4 catalysts provide much higher reusability compared to the other highly active catalysts such as Ru/Carbon black [29], Ru/CeO_2 [34], Ru/MWCNT [30], Ru/nanodiamond [49], Ru/ZrO_2 [52], Ru/HfO_2 [53], Ru/HAp [54]. Furthermore, magnetic separation of Ru^0/Fe_3O_4 and Ru^0/SiO_2-Fe_3O_4 catalysts make them advantageous over the most of the highly active catalysts given in Table 3.1.

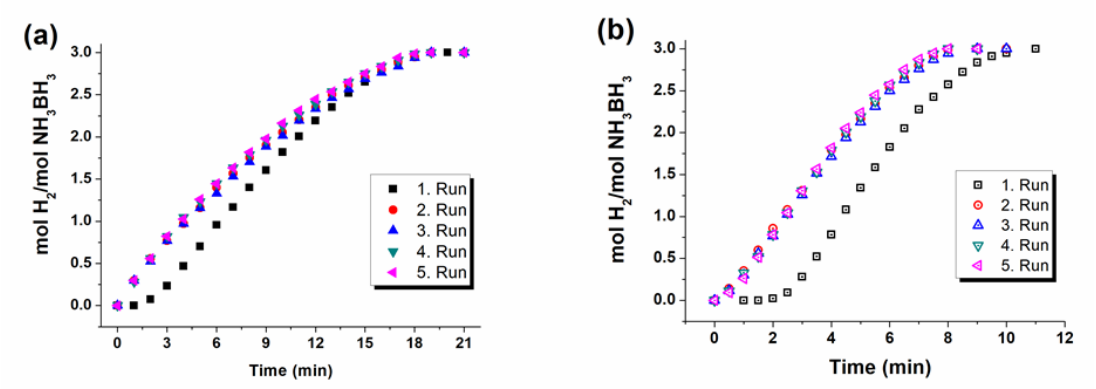

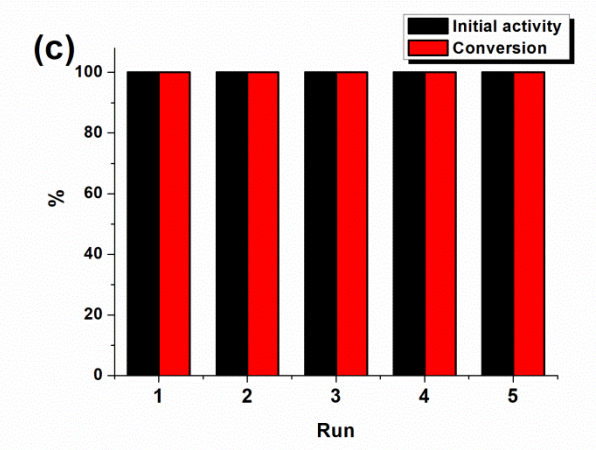

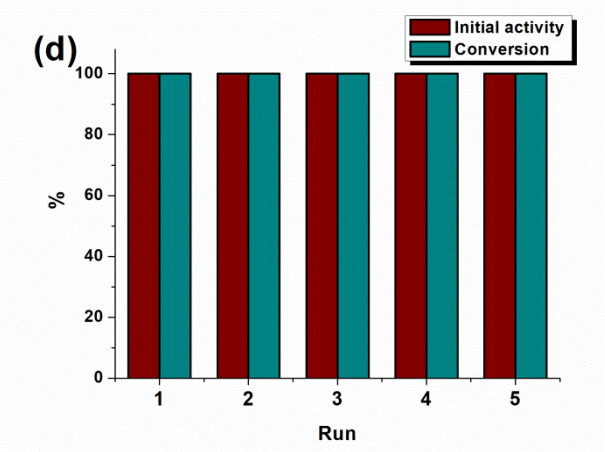

Figure 3.8. Plots of equivalent H_2 per mole of AB versus time during the successive runs of hydrolytic dehydrogenation of AB (0.10 M) starting with and (a) Ru^0/Fe_3O_4 (4.0% wt Ru; 1.18 mM Ru) (b) Ru^0/SiO_2-Fe_3O_4 (4.0% wt Ru; 1.18 mM Ru) at 25.0 ± 0.1 ºC. The corresponding percent initial catalytic activity and the percent conversion of AB for each run for (c) Ru^0/Fe_3O_4 and (d) Ru^0/SiO_2-Fe_3O_4

CHAPTER 4

CONCLUSION

The following findings and insights were obtained from this study on the development of highly active, magnetically separable and reusable ruthenium(0) nanoparticle catalysts for hydrogen generation from the hydrolysis of ammonia borane by supporting them on the surface of bare or silica coated magnetite nanopowders:

Ruthenium(0) nanoparticles were formed from the reduction of ruthenium(III) ions impregnated on the surface of bare magnetite (Ru^{3+}/Fe_3O_4) or silica coated magnetite (Ru^{3+}/SiO_2-Fe_3O_4) nanopowders with sodium borohydride in aqueous solution at room temperature. Ruthenium(0) nanoparticles could be isolated from the reaction solution by using a magnet and characterized by a combination of advanced analytical techniques. The results reveal that ruthenium(0) nanoparticles are well dispersed on the surface of bare or silica coated magnetite nanopowders.

Ruthenium(0) nanoparticles supported on the surface of bare magnetite or silica-coated magnetite nanopowders are magnetically separable nanocatalysts, which can readily be isolated from the reaction solution using a permanent magnet. Furthermore, the silica coating of magnetite nanopowders provides a remarkable increase in the catalytic activity of ruthenium(0) nanoparticles supported on the surface of silica layer compared to that on the surface of bare magnetite. Ruthenium(0) nanoparticles, supported on the surface of silica-coated magnetite, Ru^0/SiO_2-Fe_3O_4, provide a catalytic activity as high as TOF = 127 min^{-1} while the magnetite supported ruthenium(0) nanoparticles, Ru^0/Fe_3O_4 have a TOF value of 29 min^{-1} in hydrolytic dehydrogenation of ammonia borane at 25.0 ± 0.1 ºC. The huge increase in catalytic activity of magnetically separable nanocatalyst upon silica coating indicates the importance of silica layer on the surface of magnetic support. The thick silica layer

hinders the negative effect of magnetite core on the catalytic activity of ruthenium(0) nanoparticles supported on the surface of magnetite nanopowders; that is, this silica layer hinders the potential involvement of iron in the catalytic cycle. The catalytic activity of Ru^0/SiO_2-Fe_3O_4 (TOF = 127 min^{-1} at 25.0 ± 0.1ºC) is comparable with that of Ru^0/SiO_2 (TOF = 200 min^{-1} at 25.0 ± 0.1 ºC) [41]. However, the latter catalyst is not magnetically separable and, therefore, most likely not reusable as no information on its reusability has been reported in the respective paper [41]. Ru^0/SiO_2-Fe_3O_4 catalyst reported in this dissertation is magnetically separable and reusable retaining its complete initial catalytic activity even after the fifth reuse releasing 3.0 equivalent H_2 in hydrolytic dehydrogenation of ammonia borane.

The facile preparation, high catalytic activity and reusability of the magnetically separable ruthenium(0) nanoparticles in releasing 3.0 equivalent H_2 per mole of ammonia borane from the hydrolytic dehydrogenation at room temperature make them promising candidate to be considered as catalyst in the hydrogen generation systems for onboard applications.

REFERENCES

[1] International Energy Agency, OECD Green Growth Studies, 2011 www.oecd.org/greengrowth

[2] U.S Energy of Administration, Annual Energy Review, 2017, https://www.eia.gov/energyexplained/?page=us_energy_home

[3] Shahzad U. Global Warming: Causes, Effects and Solutions, Durreesamin J. 2015; 2204- 9827

[4] Perera, F. Pollution from Fossil-Fuel Combustion is the Leading Environmental Threat to Global Pediatric Health and Equity: Solutions Exist, Int. J. Env. Res. Public Health 2018; 15- 16

[5] Kunowsky M, Marco-Lozar J. P, Linares-Solano A. Material Demands for Storage Technologies in a Hydrogen Economy. J. Rev Energy, 2013; 878329: 16

[6] Energy, Technologies, issues and policies for sustainable mobility, http://www.greencarcongress.com/2017/01/20170117-hc.html

[7] Schlapbach L, Züttel A. Hydrogen-storage materials for mobile applications. Nature 2001; 414: 353- 358

[8] Züttel A. Hydrogen storage methods. Naturwissenschaften 2004; 91: 157-172

[9] Rahim A, Tijani A, Sainan I, Najmi W. An Overview of Hydrogen Production From Renewable Energy Source For Remote Area Application. Appl Mech Mater Vol. 2015; 699: 474-479

[10] Eberle U. Chemical and Physical Solutions for Hydrogen Storage. Angew. Chem. Int. Ed. 2009; 48: 6608-6630

[11] Himmelberger D. Hydrogen Release From Ammonia Borane. Publicy Accessible Penn Dissertations 2010; 158

[12] Staubitz A, Robertson APM, Manners I. Ammonia-Borane and related compounds as dihydrogen sources. Chem Rev 2010;110:4079–124.

[13] Yadav M, Xu Q. Liquid-phase chemical hydrogen storage materials. Energy Environ Sci 2012;5:9698- 725.

[14] Lin Y, Mao W. L. High-pressure storage of hydrogen fuel: ammonia borane and its related
Compound. Division of Mat. Sci. And Engineering 2009; 106: 8113-8116

[15] Umegaki T, Xu Q. Boron- and nitrogen- based chemical hydrogen storage materials. Int. J. Hydrogen Energy 2009; 24: 2303- 2311

[16] Moussa G, Moury R, Şener T, Miele P. Boron- based hydrides for chemical hydrogen storage. Int. J. Energy Res. 2013; 37:825- 842

[17] Karkamkar A, Aardahl C, Autrey T. Recent developments on hydrogen release from ammoia borane. Mater. Matters 2007; 2(6): 6-9

[18] Lu T. Nanostructure confinement of ammonia borane within porous silica and carbon for hydrogen storage. PhD thesis, James Cook University, 2010; http://researchonline.jcu.edu.au/39163/

[19] Lu Z, Yao Q, Zhang Z, Yang Y, Chen X. Nanocatalysts for hydrogen generation from ammonia borane and hydrazine borane. J. Nanomaterials 2014; 729029: 11.

[20] Jiang H, Xu Q. Catalytic hydrolysis of ammonia borane for chemical hydrogen storage. Catal Today 2011; 170: 56-63.

[21] Akbayrak S, Özkar S. Hydrogen Generation from the Hydrolysis of Ammonia Borane Using Transition Metal Nanoparticles as Catalyst, in: M. Sankır, N.D. Sankır (Eds.), Hydrogen Production Technologies, Wiley-VCH; 2017, p. 207–230.

[22] Akbayrak S, Tonbul Y, Özkar S. Ceria supported rhodium nanoparticles: Superb catalytic activity in hydrogen generation from the hydrolysis of ammonia borane. Appl. Catal. B: Environ 2016;198:162–170.

[23] Yao Q, Lu ZH, Jia Y, Chen X, Liu X. In situ facile synthesis of Rh nanoparticles supported on carbon nanotubes as highly active catalysts for H_2

generation from NH_3BH_3 hydrolysis. Int. J. Hydrogen Energy 2015;40:2207-15.

[24] Mori K, Miyawaki K, Yamashita H. Ru and Ru–Ni Nanoparticles on TiO_2 Support as Extremely Active Catalysts for Hydrogen Production from Ammonia–Borane. ACS Catal 2016;6:3128-3135.

[25] Xi P, Chen F, Xie G, Ma C, Liu H, Shao C, Wang J, Xu Z, Xu X, Zeng Z. Surfactant free RGO/Pd nanocomposites as highly active heterogeneous catalysts for the hydrolytic dehydrogenation of ammonia borane for chemical hydrogen storage. Nanoscale 2012;4:5597-5601.

[26] Akbayrak S, Özkar S. Ruthenium(0) nanoparticles supported on xonotlite nanowire: a long-lived catalyst for hydrolytic dehydrogenation of ammonia-borane. Dalton Trans 2014;43:1797–1805.

[27] Rakap M, Ozkar S. Zeolite confined palladium(0) nanoclusters as effective and reusable catalyst for hydrogen generation from the hydrolysis of ammonia-borane. Int J Hydrogen Energy 2010;35:1305-12.

[28] Yang K, Zhou L, Yu G, Xiong X, Ye M, Li Y. et al. Ru nanoparticles supported on MIL-53(Cr, Al) as efficient catalysts for hydrogen generation from hydrolysis of ammonia borane. Int. J. Hydrogen Energy 2016;41:6300-9.

[29] Liang H, Chen G, Desinan S, Rosei R, Rosei F, Ma D. In situ facile synthesis of ruthenium nanocluster catalyst supported on carbon black for hydrogen generation from the hydrolysis of ammonia-borane. Int. J. Hydrogen Energy 2012; 3:17921-27.

[30] Akbayrak S, Özkar S. Ruthenium(0) nanoparticles supported on multiwalled carbon nanotube as highly active catalyst for hydrogen generation from ammonia-borane. ACS Appl Mater Interfaces 2012;4:6302-10.

[31] Du C, Ao Q, Cao N, Yang L, Luo W, Cheng G. Facile synthesis of monodisperse ruthenium nanoparticles supported on graphene for hydrogen generation from hydrolysis of ammonia borane Int. J. Hydrogen Energy 2015;40:6180–6187.

[32] Rachiero G. P, Demirci U. B, Miele P. Bimetallic RuCo and RuCu catalysts supported on γ-Al_2O_3. A comparative study of their activity in hydrolysis of ammonia-borane. Int J Hydrogen Energy 2011; 36: 7051-65.

[33] Akbayrak S, Kaya M, Volkan M, Özkar S. Palladium(0) nanoparticles supported on silica-coated cobalt ferrite: a highly active, magnetically isolable and reusable catalyst for hydrolytic dehydrogenation of ammonia borane. Appl Catal B Environ 2014;147:387-93.

[34] Akbayrak S, Tonbul Y, Özkar S. Ceria-supported ruthenium nanoparticles as highly active and long-lived catalysts in hydrogen generation from the hydrolysis of ammonia borane. Dalton Trans. 2016;45:10969–10978.

[35] Akbayrak S, Kaya M, Volkan M, Özkar S. Ruthenium(0) nanoparticles supported on magnetic silica coated cobalt ferrite: reusable catalyst in hydrogen generation from the hydrolysis of ammonia-borane. J Mol Catal A: Chem 2014;394:253-61

[36] Hudson R, Feng Y, Varma R. S, and Moores A. Bare magnetic nanoparticles: Sustainable synthesis and applications in catalytic organic transformations. Green Chemistry 2014; 16: 4493- 4505

[37] Enthaler S, Junge K, and Beller M. Angew. Sustainable metal catalysis with iron: from rust to a rising star? Chem., Int. Ed., 2008; 47: 3317-3321

[38] Bolm C, Legros J, Paih L, and Zani L. Iron-catalyzed reactions in organic synthesis. Chem. Rev., 2004; 104: 6217-6254.

[39] Manna J, Akbayrak S, Özkar S. Palladium(0) nanoparticles supported on polydopamine coated Fe_3O_4 as magnetically isolable, highly active and reusable catalysts for hydrolytic dehydrogenation of ammonia borane. RSC Adv 2016; 6:102035-102042.

[40] Manna J, Akbayrak S, Özkar S. Nickel(0) nanoparticles supported on bare or coated cobalt ferrite as highly active, magnetically isolable and reusable catalyst for hydrolytic dehydrogenation of ammonia borane. Journal of Colloid and Interface Science 2017;508:359–368.

[41] Stöber W, Fink A. Controlled growth of monodisperse silica spheres in the micron size range. J Colloid Interface Sci 1968;26:62-9.

[42] Tonbul Y, Akbayrak S, Özkar S. Palladium(0) nanoparticles supported on ceria: Highly active and reusable catalyst in hydrogen generation from the hydrolysis of ammonia borane. Int. J. Hydrogen Energy 41 (2016) 11154-62.

[43] Chinchilla LE, Olmos CM, Villa A, Carlsson A, Prati L, Chen X. et al. Ru-modified Au catalysts supported on ceria-zirconia for the selective oxidation of glycerol. Catal Today 2015;253:178–89.

[44] Yao Q, Lu ZH, Yang K, Chen X, Zhu M. Ruthenium nanoparticles confined in SBA-15 as highly efficient catalyst for hydrolytic dehydrogenation of ammonia borane and hydrazine borane. Sci. Rep 2015;5:15186.

[45] Fan Y, Li X, He X, Zeng C, Fan G, Liu Q. et al. Effective hydrolysis of ammonia borane catalyzed by ruthenium nanoparticles immobilized on graphic carbon nitride Int. J. Hydrogen Energy 2014; 39:19982–19989.

[46] Ma Y, Li X, Zhang Y, Chen L, Wu J, Gao D, Bi J, Fan G. Ruthenium nanoparticles supported on TiO_2(B) nanotubes: Effective catalysts in hydrogen evolution from the hydrolysis of ammonia borane. J. Alloys Compd 2017;708:270–277

[47] Akbayrak S, Tanyıldızı S, Morkan İ, Özkar S. Ruthenium(0) nanoparticles supported on nanotitania as highly active and reusable catalyst in hydrogen generation from the hydrolysis of ammonia borane. Int. J. Hydrogen Energy 2014;39:9628-9637.

[48] Wen L, Su J, Wu X, Cai P, Luo W, Cheng G. Ruthenium supported on MIL-96: An efficient catalyst for hydrolytic dehydrogenation of ammonia borane for chemical hydrogen storage. Int. J. Hydrogen Energy 2014; 39:17129-35.

[49] Fan G, Liu Q, Tang D, Li X, Bi J, Gao D. Nanodiamond supported Ru nanoparticles as an effective catalyst for hydrogen evolution from hydrolysis of ammonia borane. Int. J. Hydrogen Energy 2016;41: 1542-49.

[50] Yao Q, Shi W, Feng G, Lu Z.H, Zhang X, Tao D. et al. Ultrafine Ru nanoparticles embedded in SiO_2 nanospheres: Highly efficient catalysts for hydrolytic dehydrogenation of ammonia borane. J. Power Sources 2014;257:293–299.

[51] Roy S, Pachfule P, Xu Q. High Catalytic Performance of MIL-101-Immobilized NiRu Alloy Nanoparticles towards the Hydrolytic Dehydrogenation of Ammonia Borane. Eur J Inorg Chem 2016;27:4353-57.

[52] Tonbul Y, Akbayrak S, Özkar S. Nanozirconia supported ruthenium(0) nanoparticles: Highly active and reusable catalyst in hydrolytic dehydrogenation of ammonia borane. Journal of Colloid and Interface Science 2018;513:287–294.

[53] Kalkan EB, Akbayrak S, Özkar S. Ruthenium(0) nanoparticles supported on nanohafnia: A highly active and long-lived catalyst in hydrolytic dehydrogenation of ammonia borane. Molecular Catal. 2017;430:29–35.

[54] Akbayrak S, Erdek P, Özkar S. Hydroxyapatite supported ruthenium(0) nanoparticles catalyst in hydrolytic dehydrogenation of ammonia borane: Insight to the nanoparticles formation and hydrogen evolution kinetics Appl Catal B: Environ 2013;142–143:187–195.

[55] Cao N, Hu K, Luo W, Cheng G. RuCu nanoparticles supported on graphene: A highly efficient catalyst for hydrolysis of ammonia borane. J. Alloys Compd. 2014;590:241–6.

[56] Basu S, Brockman A, Gagare P, Zheng Y, Ramachandran PV, Delgass WN, Gore J.P. Chemical kinetics of Ru-catalyzed ammonia borane hydrolysis J. Power Sources 2009;188:238–43.

[57] Cao N, Luo W, Cheng GZ. One-step synthesis of graphene supported Ru nanoparticles as efficient catalysts for hydrolytic dehydrogenation of ammonia borane. Int. J. Hydrogen Energy 2013;38:11964-72.

[58] Zhou Q, Yang H, Xu C. Nanoporous Ru as highly efficient catalyst for hydrolysis of ammonia borane Int. J. Hydrogen Energy 2016;41:12714-21.

[59] Abo-Hamed EK, Pennycook T, Vaynzof Y, Toprakcioglu C, Koutsioubas A, Scherman OA. Highly Active Metastable Ruthenium Nanoparticles for Hydrogen Production through the Catalytic Hydrolysis of Ammonia Borane. Small 2014;10:3145–52.